Visualizing Degrees of Aromaticity for Different Barbaralane Systems

Barbara Kirchner*,† and Daniel Sebastiani*,‡

Theoretical Chemistry, University of Bonn, Wegelerstraβe 12, 53115 Bonn, Germany, and Max-Planck Institute for Polymer Research, Ackermannweg 10, 55128 Mainz, Germany

Received: July 21, 2004; In Final Form: October 4, 2004

Aromaticity and homoaromaticity of a parent barbaralane and a tetraphosphabarbaralane of C_{2v}-symmetry are visualized by means of three-dimensional nucleus-independent chemical shift maps, showing the characteristic response properties of the electronic structure of these molecules. We combine this analysis with Car−Parrinello molecular dynamics simulations to incorporate the fluxional character of the tetraphosphabarbaralane and to show that atomistic motion at room temperature does not alter the aromaticity in this case.

Introduction

Aromaticity has a longstanding history as a fundamental concept in chemistry.[1] Its idea is taught in first year chemistry. The consequences range from elementary effects such as resonance stabilization up to structural driving forces of supramolecular or template assemblies and biological macromolecules. Aromaticity is often used in an intuitive way to describe electronic and structural properties of molecules. This rather cloudy use of the term aromaticity has been seeking supplementary clarification and further investigation since its first appearance.[1] After the discovery of benzene in 1825 by M. Faraday, the notion emerged roughly with the determination of its cyclic structure by Loschmidt in 1862 and Kekulé in 1865. Since then, a lot of effort has been devoted to the investigation of possible definitions of aromaticity, as well as chemical and physical properties of aromatic molecules. A vast collection of literature is available on the subject; see, for example, refs 1 and 2.

The term "homoaromaticity" was first introduced in 1959 by Winstein[3] in an attempt to describe molecules which exhibit aromatic properties while one or several common criteria of aromaticity are not satisfied, such as, for example, the need for planarity.[4,5] Many later works have used this expression to describe partly aromatic molecules. Just recently, a multidimensional aromaticity concept was suggested in this context; for further references, see refs 6−14.

Barbaralanes[15,16] are a class of polycyclic molecules (**1** in Figure 1) that undergo a degenerate Cope rearrangement reaction. The transition state (TS) between the two reactants is a conformation that has a higher symmetry (C_{2v}) than the reactants (C_s). Many extended studies[5,17−23] could confirm that an appropriate description of this transition state is homoaromatic **1***, rather than biradicaloid or radicaloid. Several experimental as well as theoretical studies have aimed at finding a possible candidate for which the double-minimum ground-state potential energy surface is turned into a single-minimum potential with the molecule exhibiting higher symmetry,[21,24,25] that is, reducing the barrier of the transition state such that it becomes a stable state. Whereas so far no gas-phase stable nondegenerate ground-state barbaralane could be determined in experiment, Seefelder and Quast received such a candidate employing different solvents.[20] They showed that dipolarity/polarizability and the electron pair donation ability of the solvents play the predominant role. Furthermore, very interesting extended barbaralanes giving rise to through-space interactions were suggested by Tantillo et al.[26] Additionally, barbaralanes and the thermochromic properties of similar molecules were investigated with respect to their use as molecular switches.[20,27] Recently, one of the present authors (B.K.) suggested a homoaromatic barbaralane (**3**) in a theoretical work[19] using an isolated molecule ansatz. Applying static quantum chemistry geometry optimization, the tetraphosphabarbaralane (**3**) displayed C_{2v}-symmetry, that is, a nondegenerate minimum structure instead of C_s-symmetry, which is a degenerate minimum structure. The barrier for the Cope rearrangement of the corresponding parent-barbaralane (**1**) agreed very well with experiment in the previous study,[19] supporting the applicability of the chosen methods.

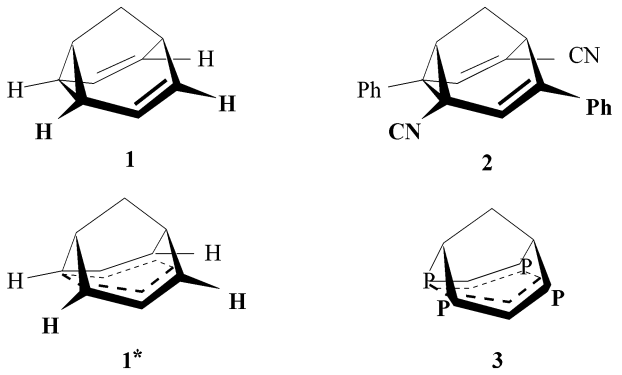

Figure 1. First column: barbaralane **1** and the symmetrical transition state **1***. Second column: diphenyl-dicyano-barbaralane **2** and tetraphosphabarbaralane **3**.

In the present investigation, we are aiming at a further characterization of **3**. The focus is three-dimensional nucleus-independent chemical shift (NICS) maps.[28] Here, we study NICS maps of aromatic, nonaromatic, and homoaromatic compounds to contribute to the characterization of homoaromaticity in general. We use this study then as a basis for a discussion of

* Corresponding authors. E-mail: kirchner@thch.uni-bonn.de (B.K.); sebastia@mpip-mainz.mpg.de (D.S.).
† University Bonn.
‡ Max-Planck Institute for Polymer Research.

10.1021/jp0467705 CCC: $27.50
Published on Web 12/07/2004

the characteristics of the previously proposed C_{2v}-symmetrical barbaralane **3**.[19] Additionally, we expose this barbaralane to a dynamical ansatz to model finite temperature effects. In particular, we will investigate the question of whether NICS maps can help to characterize the fluxional character of **3** at room temperature by combining NICS with a Car−Parrinello molecular dynamics (CPMD) simulation.[29] In CPMD simulations, the electronic structure of a system is calculated "on the fly" along a molecular dynamics trajectory. Polarization effects are explicitly included, and the pairwise additivity as used in almost all force field based molecular dynamics simulations is circumvented. The access to the electronic structure during a CPMD simulation allows the calculation of averaged electronic properties. Through an appropriate transformation of the Kohn−Sham orbitals, maximally localized Wannier functions can be calculated. Wannier orbitals[30] are the condensed phase analogues of localized molecular orbitals known from quantum chemistry. They give insight into the nature of chemical bonds and aid in the understanding of chemical concepts (e.g., nonbonding electron pairs or valency). Recent applications of the maximally localized Wannier functions are the calculations of IR absorption,[31−33] of Raman spectra,[34] and of NMR chemical shifts.[35]

Methods

Nucleus-independent chemical shift is a generalization of the atom-specific chemical shift, defined as the trace of the shielding tensor relative to a reference molecule.[28] NICS shows how much the chemical shift of a fictitious nuclear spin, located at a specific position in the neighborhood of the investigated molecule, would be changed. It was first introduced by Schleyer as a "simple and efficient aromaticity probe"[28] in 1996. Schleyer and co-workers proposed to use the absolute magnetic shielding calculated at ring centers to determine aromaticity. Negative "nucleus-independent shifts" (NICSs) indicate aromaticity, while positive NICS values denote antiaromaticity. Recently, this quantity was applied to investigate possible neutral bishomoaromatic semibullvalenes and barbaralanes.[17] One of the present authors (D.S.) applied three-dimensional NICS maps, that is, by means of isosurface plots or slices, to a supramolecular assembly of dendritic polymers.[36] This approach which has been previously examined[28,37,38] has the advantage that the NICS values are computed at every point in space, as opposed to a discrete set of isolated special points.

In all calculations, the framework of density functional theory employing the BP86 functional was used.[39,40] For the molecular dynamics calculations as well as the geometry optimizations, we applied the CPMD code.[41] We used Troullier−Martins norm-conserving pseudopotentials[42] in the Kleinman−Bylander scheme[43] together with a 70 Ryd plane wave cutoff. To enable the study of isolated systems, the inherent periodicity of the plane-wave calculations was circumvented by applying an appropriate Poisson solver designed for nonperiodic boundary conditions.[44] The cell size was set to 14 Å^3, which was found to be sufficient to converge the energies and geometries with respect to the cell parameters. We equilibrated the system for about a picosecond at 320 K with a chain of Nosé−Hoover thermostats coupled to the ionic degrees of freedom,[45,46] before starting a production run of another picosecond at the same temperature. A 3.0 au time step (1 au = 0.0242 fs) in combination with a 400 au fictitious electron mass was chosen. These values recently were shown to be carefully chosen for obtaining good structural and dynamical properties.[47]

The calculation of NICS maps was done by density functional perturbation theory[48] as implemented in the CPMD code,[41] which is an extension to the NMR chemical shift module.[49] Technically, we calculate the electronic current density, which is the linear response to an external magnetic field applied to the system.[50]

This quantum current induces an additional inhomogeneous magnetic field in the environment of the charge distribution. We compute this inhomogeneous field at all points of space. The resulting three-dimensional plot is visualized by a color scheme (see Figures 2, 3, and 5) in which the blue to yellow color means that the external field is attenuated, whereas it is reinforced in red regions. The delocalized character of typical aromatic electrons is translated into particularly large blue/yellow areas above and below the aromatic plane. This is due to the extended flexibility of the electrons; metaphorically speaking, they can create more extended "ring currents" than if they were aliphatic. Another feature of aromatic electron systems is a small area of opposite effect, that is, where the external field is increased (red color code). The shape of both of these effects can be seen in the nucleus-independent chemical shifts. The color scheme in the figures is gauged in parts per million (ppm), which designates the dimensionless proportionality coefficient between the induced and the external magnetic field. A charge-free test spin located at a given position in space would experience a displacement in its NMR chemical shift of the corresponding NICS value at that position. Working with a plane wave basis set, the calculation of all relevant quantities in the entire supercell is straightforwardly done by means of fast Fourier transformations.

Results: NICS Maps for Aromatic Molecules

In the original work of Schleyer and co-workers,[28] several test molecules were examined to assess the NICS method. For instance, a calculation employing a 6-31+G* basis set and the functional B3LYP[28] gave a value of −9.7 for benzene and −2.2 for cyclohexane, marking therefore a simple characteristic of distinguishing nonaromaticity from aromaticity. In our calculations, the aromatic systems exhibit large and long-ranged π-shifts in the neighborhood of the electrons, whereas the nonaromatic systems show restricted areas as can be seen in Figure 2, where the (aromatic) ring of atoms lies perpendicular to the plane.

In Figure 2, we have depicted NICS maps for representative aromatic, homoaromatic, and nonaromatic molecules: cyclopropane and dihydroxy-cyclopropenone (nonaromatic), the cyclopropenyl cation (aromatic), and the tris-homocyclopropenyl cation (homoaromatic). The maps of these molecules exhibit a very characteristic shape, which can be associated in a straightforward way with their aromaticity classification. As expected, the characteristic π-shifts (to lower frequencies, indicated in blue and yellow areas) are seen above and below an aromatic moiety, whereas the inverse effect can be found in a small localized region (a torus) beside the ring (indicated in orange/red areas). Note the remarkable spatial extension of the shielding effect. Even at a distance of about 3 Å, there is still a NICS displacement of more than 0.5 ppm. Regarding cyclopropane, we see that the aliphatic compound exposes significantly smaller shielding zones than the aromatic molecule. In addition, there is no deshielding effect next to the cyclopropane ring.

For the homoaromatic tris-homocyclopropenyl cation, we are able to pin down a sizable difference to the nonaromatic compound by means of the larger π-shifted area. Thus, we can assign a more aromatic behavior to this system. However, we cannot unequivocally assign the aromatic behavior to one of the rings, because there is a yellow cone below and above each

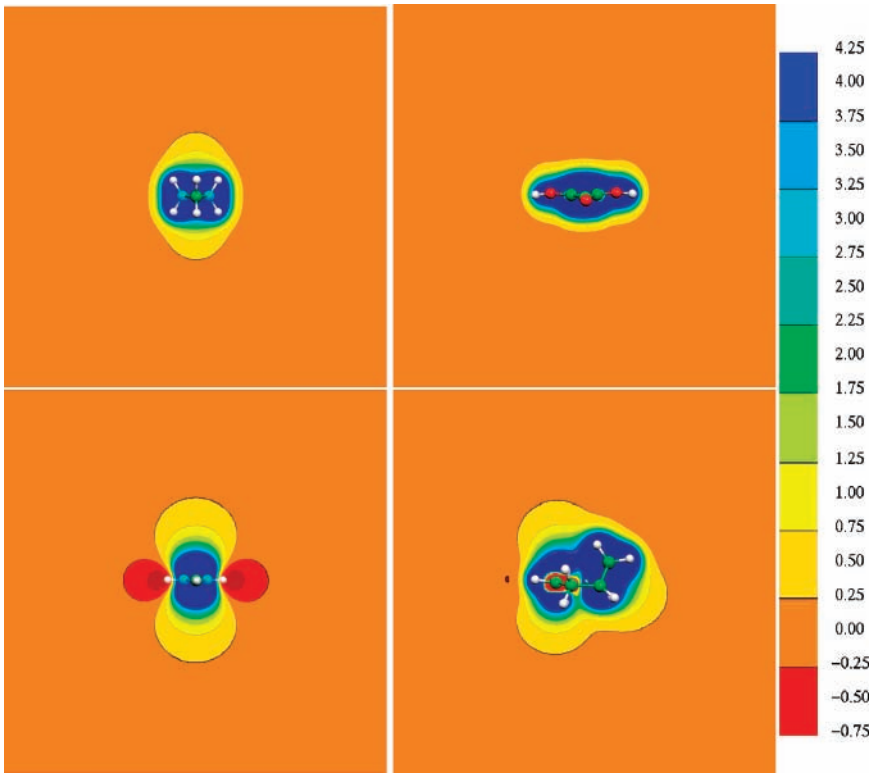

Figure 2. NICS maps for non-, homo-, and aromatic molecules. Top: cyclopropane (left) and dihydroxy-cyclopropenone (right). Bottom: cyclopropenyl cation (left) and tris-homocyclopropenyl cation (right). The spatial extension of the positive shift regions (yellow) is significantly larger for the homoaromatic (bottom right) and aromatic (bottom left) molecules than for the aliphatic ones. Note also the negative shift areas (red) outside the ring of the aromatic cyclopropenyl cation. Units in the color scheme are ppm (parts per million).

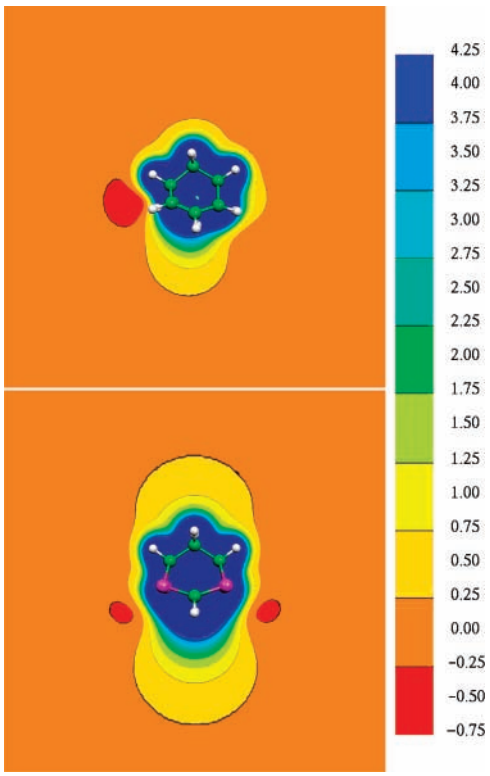

Figure 3. NICS maps for the two barbaralanes in their ground-state minimum structure. Top: **1**. Bottom: **3** (see Figure 1).

ring. Furthermore, our calculations do not display a chair structure as suggested by the Lewis formula (one 6-ring with alternating sp^2-sp^3 carbon atoms, the sp^2 carbons forming a homoaromatic 3-ring submoiety). Instead, we get one three-membered ring (with tetragonally coordinated carbons) sharing

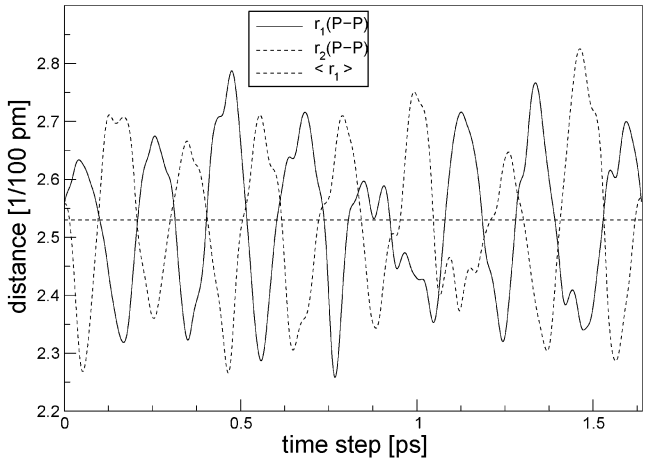

Figure 4. The evolution of the phosphorus−phosphorus atom distances of compound **3** with simulated time in picoseconds (ps).

one bond with a 5-ring, which is long known to be the right structure; see, for example, the NMR measurements by Winstein.[51] These adjustments to aromatic and nonaromatic test molecules are also in accordance with the very recent work of Merino et al.,[38] which was published after submission of this Article. These authors compared, for example, benzene with cyclohexane among other molecules.

Turning now to NICS maps for the two barbaralane molecules (**1** and **3**) in their optimized geometry (Figure 3), we find that barbaralane **1** has only one small characteristic area under the cage, and nothing is observed above. This region concentrates beneath the two localized double bonds in the ring and reflects the more asymmetrical structure (C_s) of **1** as compared to the tetraphosphabarbaralane **3** (C_{2v}). The NICS map of the latter is found to be very similar to that of the aromatic cyclopropenyl

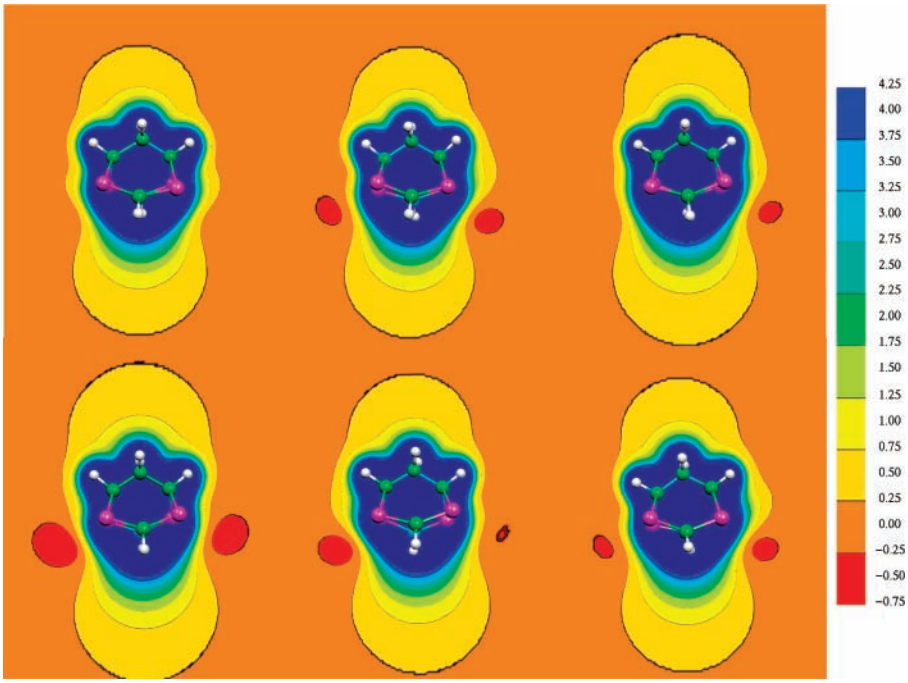

Figure 5. Time evolution of the NICS maps of **3** during a Car−Parrinello molecular dynamics trajectory. The geometries are selected configurations characteristic for the different stages of the Cope rearrangement (order: from top left to top right, then bottom left to bottom right). Note the motion of the red areas, which are typical for aromatic molecules, from one P−P bond to the other. A large aromaticity which disappears again, corresponding to extended red areas, is found when the P−P distance is below 2.6 Å.

cation shown in Figure 2 with long-ranged π-shifts below and above the cyclic structure. Also, the typical red features on the lateral sides are present. Thus, the tetraphosphabarbaralane possesses more aromatic character than the parent barbaralane **1** and the tris-homocyclopropenyl cation, and it is thus a better candidate to study homoaromaticity. These results are in accordance with Schleyer's work about semibullvallenes, barbaralanes, and bullvallenes.[17] Comparing the ground-state (C_s) NICS = −8.3 ppm with the transition state (C_{2v}) NICS = −21.5 ppm for barbaralane **1**, clearly a more aromatic character for a C_{2v} minimum structure is to be expected.

In extension to the statical picture, we also studied the dynamical behavior of **3**. Figure 4 shows the evolution of P−P distances, of the phosphorus atoms which are next to each other, of **3** in the Car−Parrinello simulation at finite temperature (T = 320 K). We see that the structure changes from the form with C_s-symmetry over the geometry of C_{2v}-symmetry to the mirrored structure of C_s-symmetry. During 1 ps of molecular dynamics (MD), nine Cope rearrangement analogous vibrations of **3** are observed. On average, one such event takes about 0.22 ps, so that the estimated wavenumber of this mode is roughly 150 cm^{-1}. The harmonic frequency analysis of the geometry-optimized molecules shows modes at about 162 cm^{-1}, which move in line with the Cope rearrangement.[19] Thus, it appears justified to characterize this process as a vibrational mode, rather than a proper chemical reaction between two well-defined reactants which are separated by a significant energy barrier.

Further clarification is given by the time evolution of the NICS maps for the tetraphosphabarbaralane that are shown in Figure 5.

Although the geometric parameters undergo large changes during the Cope rearrangement-like vibration, no significant change in the NICS maps is observed. The central features, that is, the large aromaticity-indicating cones above and below the molecule, are conserved during the CPMD simulation. The inversely π-shifted regions are small and disappear temporarily, which is an indication for the somewhat weaker aromatic character of the system. However, the comparison with nonaromatic species, as shown in Figure 2, proves the undoubtedly aromatic properties of the tetraphosphabarbarlane at ambient temperature. We thus conclude that the term homoaromaticity can definitively be applied to this molecule. In particular, its homoaromaticity is not altered when switching from the $T = 0$ K description to the more realistic finite temperature simulation.

Conclusion

We presented in this Article calculations with our NICS implementation in a CPMD framework for different test molecules. We confirmed the applicability of so-called NICS maps for distinguishing between nonaromatic, homoaromatic, and aromatic molecules. Our results are in excellent agreement with previous suggested mapping schemes.[28,37,38] For the problem of determining aromaticity and homoaromaticity, we could show gradual differences by depicting static NICS maps for a C_s-symmetrical barbaralane and a C_{2v}-symmetrical barbaralane. These results are in accordance with the work of Schleyer and co-workers on this subject.[17]

With the present implementation at hand, we were able to study the aromaticity issue for molecules at finite temperature, instead of at zero temperature as in previous studies. Our approach thus resembles the experimental situation much better than static quantum chemical calculations. Thus, the major point of this study is that we extended the NICS maps to a dynamical regime and applied this option to the previously suggested tetraphosphabarbaralane with C_{2v}-symmetry. We were able to characterize its behavior under finite temperature. Because the tetraphosphabarbaralane undergoes large geometrical changes in the phosphorus atom−phosphorus atom distance (30−40 pm) under the influence of temperature and these movements are in line with a Cope rearrangement, the question arose as to whether this molecule exhibiting time-dependent C_s-symmetry also changes its aromatic character largely. With the help of NICS maps, we could confirm that it stays aromatic, and we can thus

appraise that the term homoaromatic for the C_{2v}-state of barbaralanes is appropriate.

Acknowledgment. D.S. acknowledges financial support from the Deutsche Forschungsgesellschaft (DFG) under research grant SE 1008/2 and wishes to thank the Otto-Röhm foundation for the allocation of a generous research support. B.K. acknowledges financial support from the Deutsche Forschungsgemeinschaft (DFG) of the Sonderforschungsbereich 624 and the Forschungskredit of the University of Zürich.

References and Notes

(1) Minkin, V. M. N. G.; Simkin, B. Y. *Aromaticity and Antiaromaticity: Electronic and Structural Aspects*; Wiley−Interscience: New York, 1994.
(2) von Ragué Schleyer, P., Ed. *Aromaticity* **2001**, *101*.
(3) Winstein, S. *J. Am. Chem. Soc.* **1959**, *81*, 6524−6525.
(4) Williams, R. V.; Kurtz, H. *Adv. Phys. Org. Chem.* **1994**, *29*, 273.
(5) Williams, R. V. *Chem. Rev.* **2001**, *101*, 1185−1204.
(6) Jemmis, E. D.; von Ragué Schleyer, P. *J. Am. Chem. Soc.* **1982**, *104*, 4781−4788.
(7) Haddon, R. C. *Acc. Chem. Res.* **1988**, *21*, 243−249.
(8) Katritzky, A. R.; Barczynski, P.; Musumarra, G.; Pisano, D.; Szafran, M. *J. Am. Chem. Soc.* **1989**, *111*, 7−15.
(9) Jug, K.; Köster, A. M. *J. Phys. Org. Chem.* **1991**, *4*, 163−169.
(10) Krygowski, T. M.; Ciesielski, A.; Bird, C. W.; Kotschy, A. *J. Chem. Inf. Comput. Sci.* **1995**, *35*, 203−210.
(11) Neus, J. *Studies in History and Philosophy of Chemistry*; HYLE Publications: Karlsruhe, 2002; Vol. 2, www.hyle.org/publications.
(12) Chen, Z.; Jiao, H.; Hirsch, A.; von Ragué Schleyer, P. *Angew. Chem.* **2002**, *114*, 4485−4488.
(13) Chen, Z.; Jiao, H.; Hirsch, A.; von Ragué Schleyer, P. *Angew. Chem., Int. Ed.* **2002**, *41*, 4309−4312.
(14) Reiher, M.; Hirsch, A. *Chem.-Eur. J.* **2003**, *9*, 5442−5452.
(15) v. E. Doering, W.; Roth, W. R. *Angew. Chem.* **1963**, *75*, 27−35.
(16) v. E. Doering, W.; Roth, W. R. *Angew. Chem., Int. Ed. Engl.* **1963**, *2*, 115−122.
(17) Wu, H.; Jiao, H.; Wang, Z.; v. R. Schleyer, P. *J. Am. Chem. Soc.* **2003**, *125*, 10524−10525.
(18) Staroverov, V. N.; Davidson, E. R. *J. Am. Chem. Soc.* **2000**, *122*, 186−187.
(19) (a)Reiher, M; Kirchner, B. *Angew. Chem., Int. Ed.* **2002**, *41*, 3429−3583 (b)Reiher, M.; Kirchner, B. *Angew. Chem.,* **2002**, *114*, 3579−3583.
(20) Seefelder, M.; Quast, H. *Angew. Chem., Int. Ed.* **1999**, *38*, 1068−1072.
(21) Jackman, L. M.; Fernandes, E.; Heubes, M.; Quast, H. *Eur. J. Org. Chem.* **1945**, *10*, 2209−2227.
(22) Gompper, R.; Nöth, H.; Spes, P. *Tetrahedron Lett.* **1988**, *29*, 3639−3642.
(23) Dewar, M. J. S.; Lo, D. H. *J. Am. Chem. Soc.* **1971**, *93*, 7201−7207.
(24) Chen, Y.; Hartmann, M.; Diedenhofen, M.; Frenking, G. *Angew. Chem., Int. Ed.* **2001**, *40*, 2051−2055.
(25) Chen, Y.; Hartmann, M.; Diedenhofen, M.; Frenking, G. *Angew. Chem.* **2001**, *113*, 2107−2112.
(26) Tantillo, D. J.; Hoffmann, R.; Houk, K. N.; Warner, P. M.; Brown, E. C.; Henze, D. K. *J. Am. Chem. Soc.* **2004**, *126*, 4256−4263.
(27) Dohle, M.; Manz, J.; Paramonov, G. K.; Quast, H. *Chem. Phys.* **1995**, *197*, 91−97.
(28) v. R. Schleyer, P.; Maerker, C.; Dransfeld, A.; Jiao, H.; v. E. Hommes, N. J. R. *J. Am. Chem. Soc.* **1996**, *118*, 6317−6318.
(29) Car, R.; Parrinello, M. *Phys. Rev. Lett.* **1985**, *55*, 2471−2474.
(30) Wannier, G. *Phys. Rev.* **1937**, *52*, 191.
(31) Bernasconi, M.; Silvestrelli, P.-L.; Parrinello, M. *Phys. Rev. Lett.* **1998**, *81*, 1235−1238.
(32) Gaigeot, M.-P.; Sprik, M. *J. Phys. Chem. A* **2003**, *107*, 10344−10358.
(33) Kirchner, B.; Hutter, J. *J. Chem. Phys.* **2004**, *121*, 5133−5142.
(34) Putrino, A.; Parrinello, M. *Phys. Rev. Lett.* **2002**, *88*, 176401.
(35) Sebastiani, D.; Parrinello, M. *ChemPhysChem* **2002**, *3*, 675.
(36) Rapp, A.; Schnell, I.; Sebastiani, D.; Brown, S. P.; Percec, V.; Spiess, H. W. *J. Am. Chem. Soc.* **2003**, *125*, 13284−13297.
(37) Klod, S.; Koch, A.; Kleinepeter, E. *J. Chem. Soc., Perkin Trans.* **2002**, *2*, 1506−1509.
(38) Merino, G.; Heine, T.; Seifert, G. *Chem.-Eur. J.* **2004**, *10*, 4367−4371.
(39) Becke, A. D. *Phys. Rev. A* **1988**, *38*, 3098−3100.
(40) Perdew, J. P. *Phys. Rev. B* **1986**, *33*, 8822−8824.
(41) "CPMD V3.8 Copyright IBM Corp. 1990−2003, Copyright MPI für Festkörperforschung Stuttgart 1997−2001", see also www.cmpd.org.
(42) Troullier, N.; Martins, J. L. *Phys. Rev. B* **1991**, *43*, 1993.
(43) Kleinman, L.; Bylander, D. M. *Phys. Rev. Lett.* **1982**, *48*, 1425.
(44) Martyna, G.; Tuckerman, M. *J. Chem. Phys.* **1999**, *110*, 2810.
(45) Nosé, S. *Mol. Phys.* **1984**, *5*, 255.
(46) Hoover, W. G. *Phys. Rev. A* **1985**, *31*, 1695.
(47) Marx, D.; Hutter, J. Ab initio Molecular Dynamics: Theory and Implementation. *Modern Methods and Algorithms in Quantum Chemistry*; Forschungzentrum Juelich: 2000; Vol. 1.
(48) Putrino, A.; Sebastiani, D.; Parrinello, M. *J. Chem. Phys.* **2000**, *113*, 7102.
(49) Sebastiani, D.; Parrinello, M. *J. Phys. Chem. A* **2001**, *105*, 1951.
(50) Sebastiani, D.; Goward, G.; Schnell, I.; Spiess, H.-W. *J. Mol. Struct. (THEOCHEM)* **2003**, *625*, 283−288.
(51) Lowry, T. H.; Richardson, K. S. *Mechanism and theory in organic chemistry*; Harper: New York, 1986.